

Increased resolution and penetration from a towed dual-sensor streamer

David Carlson¹, Andrew Long², Walter Söllner¹, Hocine Tabti,¹ Rune Tenghamn,³ and Nils Lunde³ discuss the theory behind a towed dual-sensor developed by Petroleum Geo-Services to operate at deeper depths and deliver de-ghosted data.

A pressure sensor in a towed streamer always records two wavefields that interfere with each other. The two wavefields are the up-going pressure wavefield propagating directly to the pressure sensor from the earth below and the down-going pressure wavefield reflected downwards from the free (sea) surface immediately above the streamer. Thus, every recorded reflection wavelet from conventional marine streamers is accompanied by a ghost reflection from the ocean's surface. The reflection wavelet is undesirably elongated, reducing temporal resolution. The consequence, as illustrated in Figure 1a (vertical wavefield propagation with zero incidence angle), is that a series of receiver 'ghost' notches are introduced into the frequency spectra. For zero angle reflections the frequency of notches is always at 0 Hz and integer multiples of $\frac{V_w}{2d}$, where V_w is the velocity of sound in water, and d is the receiver depth. This filter effect on the recorded data has restricted streamer towing depths to a range of about 6-9 m. A deeper towing depth would be desirable as it would improve the recording of the lower frequencies in addition to placing the seismic sensors farther below weather induced surface wave noise. However,

this will have a destructive effect on the higher frequencies of the recorded signal because of the ghost notch moving to lower frequencies (Figure 1a). The trade-off between low and high frequencies forces the geoscientist to parameterize streamer surveys to maximize data quality at one target depth, whilst sacrificing image quality at shallower or deeper targets.

It has long been understood that by sensing and recording seismic data from collocated hydrophones and velocity sensors, and by properly combining their signals, ghost reflections can be cancelled (Schneider and Backus, 1964; Claerbout, 1976). A new solid core dual-sensor cable has been introduced that simultaneously measures the pressure using hydrophones and the vertical component of the particle velocity using motion sensors (Tenghamn et al., 2007). For each type of measurement, the water surface reflections (ghosts) impose a filter on the data (Figure 1b). In contrast to pressure sensors, however, velocity sensors are directional, so the down-going velocity wavefield is measured as having equal polarity to the up-going velocity wavefield. Consequently, as observed in Figure 1b, receiver ghost notches for

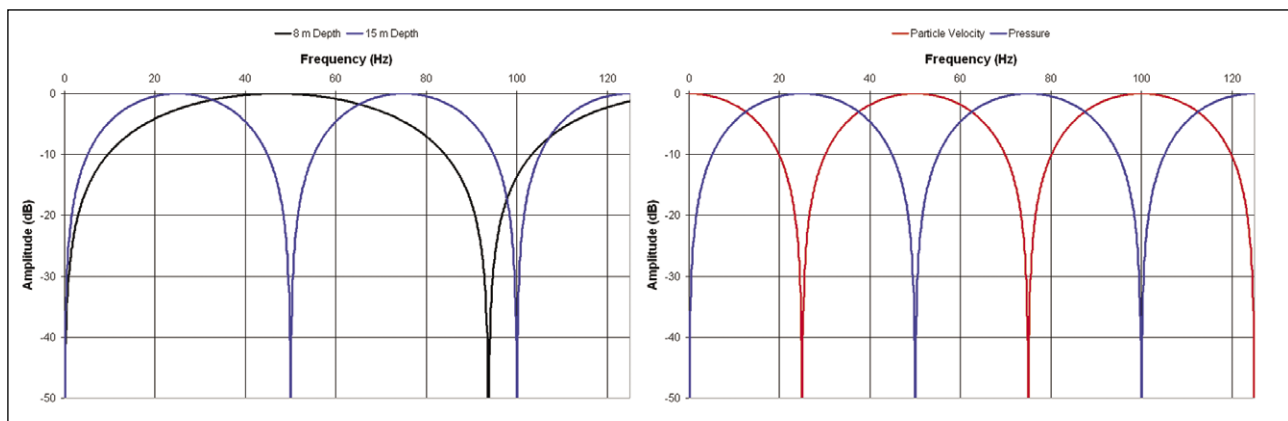


Figure 1 The image on the left shows the receiver amplitude spectra for a pressure sensor towed at 8 m and 15 m depth. The wavefield is assumed to have vertical propagation (zero angle of incidence). Black is 8 m receiver depth, and blue is 15 m receiver depth. The image on the right shows the superposition of the amplitude spectra for both the pressure and velocity sensor at 15 m depth for zero angle reflections. Blue is the pressure wavefield spectra, and red is the velocity wavefield spectra.

¹ Petroleum Geo-Services, Oslo, Norway. E-mail: dave.carlson.pgs.com.

² Petroleum Geo-Services, Perth, Australia.

³ Petroleum Geo-Services, Houston, USA.

Marine Seismic

the velocity sensor are still separated by integer multiples of $\frac{V_w}{2d}$, but are offset by $\frac{V_w}{4d}$ from the hydrophone spectra.

Four aspects are important to note when considering the receiver ghosts for dual-sensor data:

- The peaks and notches in the amplitude spectra for pressure data are complementary to those for velocity data (Fig. 1b).
- The ‘proper’ summation of pressure and velocity data will cancel the amplitude of the ghost event (down-going wavefield from the sea surface) trailing each primary event, and the notches in the amplitude spectra will be removed. This is the case for all angles of incidence, i.e. for all source-receiver offsets.
- The ‘opposite’ summation will give the down-going reflections from the sea surface which contain information about the sea state that is very useful for subsequent processing such as surface-related multiple elimination, as will be shown below.
- The wavefield separation recovers significant low and high frequency amplitudes normally missing from conventional marine seismic data.

Figure 2 is a simple synthetic example that conceptually demonstrates the summation of zero-offset stacks for pressure and velocity data from a dual-sensor streamer. The receiver ghost that complicates interpretation of relatively thick intervals is removed by summation, and a clear image results.

The advantages of measuring both the pressure and vertical particle velocity wavefields in this manner are numerous.

Operationally, it is attractive to tow as deep as possible, as weather and operational noise are minimal, the streamers are better behaved, and signal penetration for low frequencies is optimized. As discussed below, the availability of particle velocity measurements allows deep towing, whilst simultaneously acquiring high amplitude low and high frequencies – with improved signal-to-noise ratio (Carlson et al., 2007). The new streamer uses a quiet, ruggedized solid streamer design to deliver de-ghosted data in one pass, using one streamer depth. The up- and down-going wavefields can be extrapolated and summed to reconstruct the total wavefield at any desired recording depth to duplicate the parameters of any existing survey, thus allowing 4D matching plus the benefits of improved image clarity.

Dual-sensor streamer theory

If the vertical component of particle velocity is measured together with the pressure field, the seismic wavefield can be decomposed in data processing into the up-going and down-going pressure and velocity wavefields (e.g. Schneider and Backus, 1964; Claerbout, 1976; Barr and Sanders, 1989; Amundsen, 1993; Fokkema and van den Berg, 1993). The inversion of a function with a notch in the frequency spectrum is completely avoided. Furthermore, the shape of the sea surface is irrelevant, and the streamer may be towed at any depth. The source wavelet may also be derived from the de-ghosted data, allowing the implementation of sophisticated de-multiple routines.

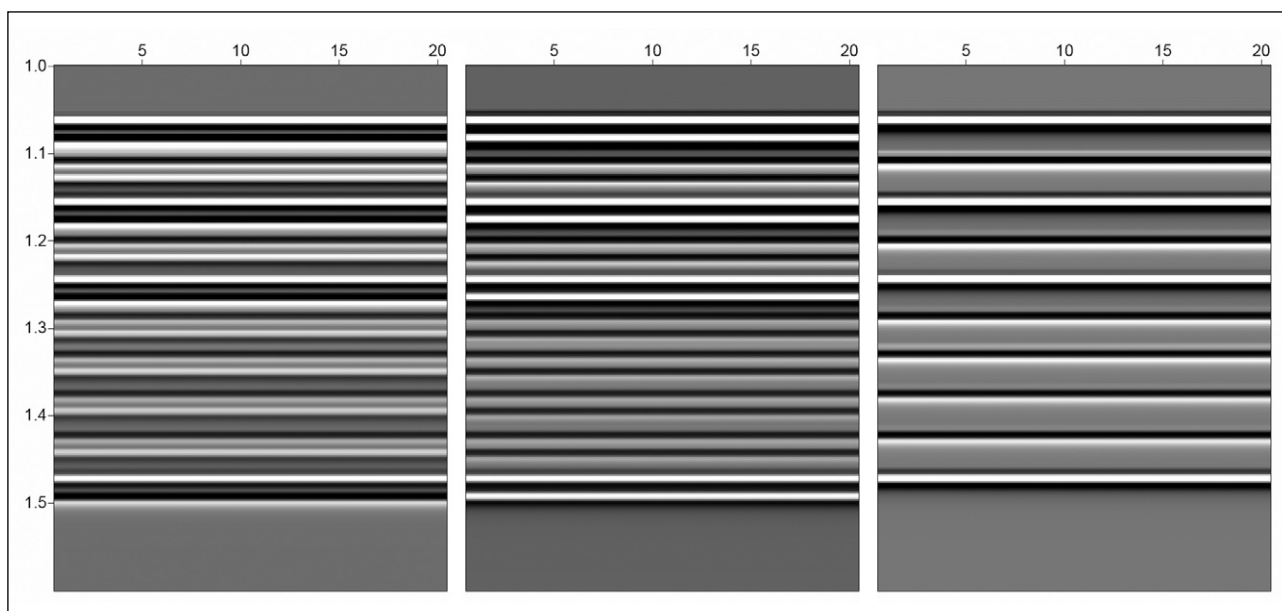


Figure 2 Conceptual synthetic zero-offset stacks for pressure-only, velocity-only, and summation of pressure+velocity, respectively. The arrival time of primary and receiver ghost events is identical for both pressure and velocity. The polarity of primary events is identical for pressure and velocity, but the polarity of receiver ghost events is opposite. Summation cancels the receiver ghost present in the pressure and velocity data.

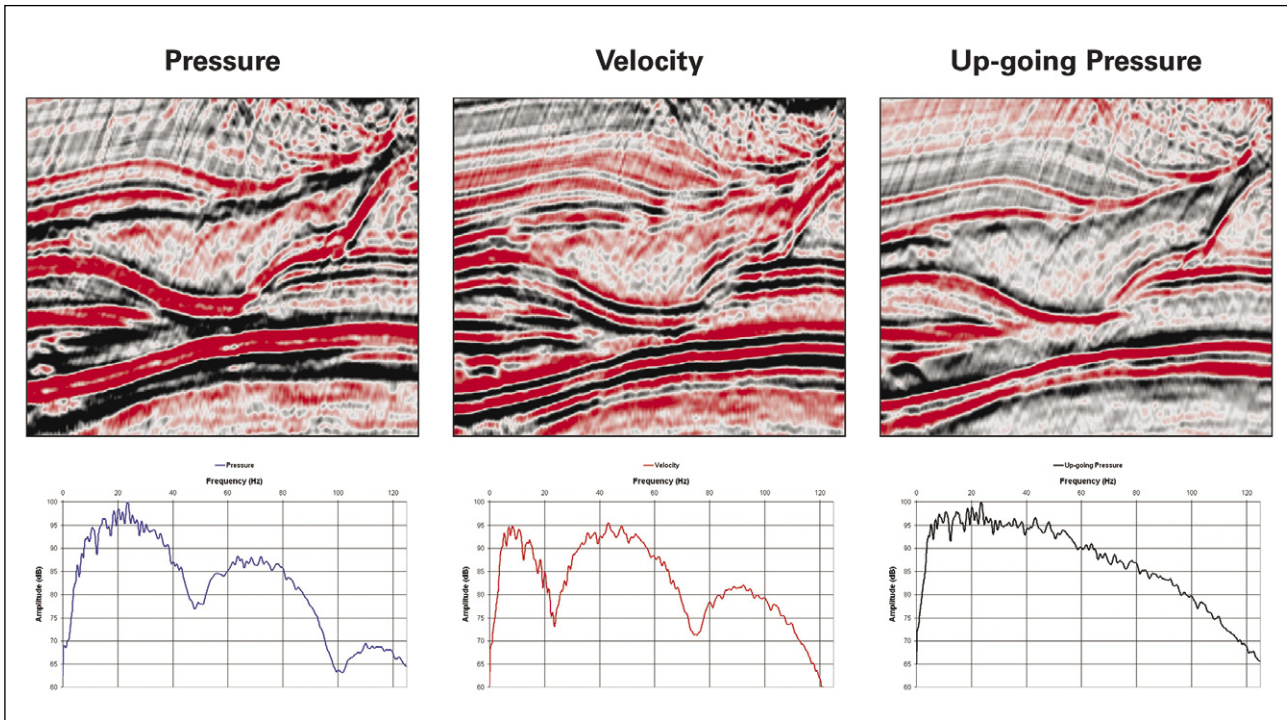


Figure 3 Unmigrated stack comparison. Note the complementary amplitude spectra for pressure vs. particle velocity (refer also to Fig. 1). The images are from left to right, the pressure-only result, the (vertical) velocity-only result, and the up-going (de-ghosted) pressure wavefield derived from the pressure and velocity wavefields.

In the frequency wavenumber domain the up-going and down-going pressure wavefields are related to the pressure and the vertical component of the particle velocity by the following matrix equation:

$$\begin{bmatrix} U \\ D \end{bmatrix} = \frac{1}{2} \begin{bmatrix} 1 & -\frac{\rho\omega}{k_z} \\ \frac{\rho\omega}{k_z} & 1 \end{bmatrix} \begin{bmatrix} P \\ V_z \end{bmatrix},$$

where k_z is the vertical wavenumber and the positive z -axis is downwards.

An example of wavefield separation is shown in Figure 3. This example is taken from a survey with 6100 m streamer length. Both the pressure and velocity data were recorded with collocated sensors at a depth of 15 m. Extraction of the (de-ghosted) up-going pressure wavefield followed the principles discussed above.

In a homogeneous medium the vertical pressure gradient is related to the vertical component of the particle velocity V_z through the equation of motion as follows:

$$\frac{dP}{dz} = i\omega\rho V_z,$$

where $\omega = 2\pi f$ is circular frequency, and ρ is density.

In the frequency wavenumber domain, the solution for the vertical component of the particle velocity is given by:

$$V_z(\omega, k_x, k_y, z) = -\frac{k_z}{\rho\omega} \left[\frac{\exp(-ik_z z) + \exp(ik_z z)}{\exp(-ik_z z) - \exp(ik_z z)} \right] \times P(\omega, k_x, k_y, z),$$

where k_x , k_y , and k_z are the two horizontal and vertical wave numbers, respectively, and z is the receiver depth. This equation is valid for flat streamers and a flat sea surface, and assumes that the direct arrivals have been removed.

The data examples shown in this paper correspond to 2D acquisition, and consequently a 2D assumption has been made in data processing, however the extension to 3D processing is straightforward.

Acquisition and processing of dual-sensor data

The dual-sensor acquisition described here represents the first successful implementation of a dual-sensor towed marine streamer system. The efficient architecture uses densely sampled groups of collocated pressure and velocity sensors in a low-noise solid-fill streamer with distributed electronics and Ethernet telemetry. The system provides significantly increased flexibility in streamer towing depth allowing continued recording in rough seas, while increasing the potential bandwidth of the data. In the examples shown here the dual-sensor streamer was typically towed at a depth of 15 m. At

Marine Seismic

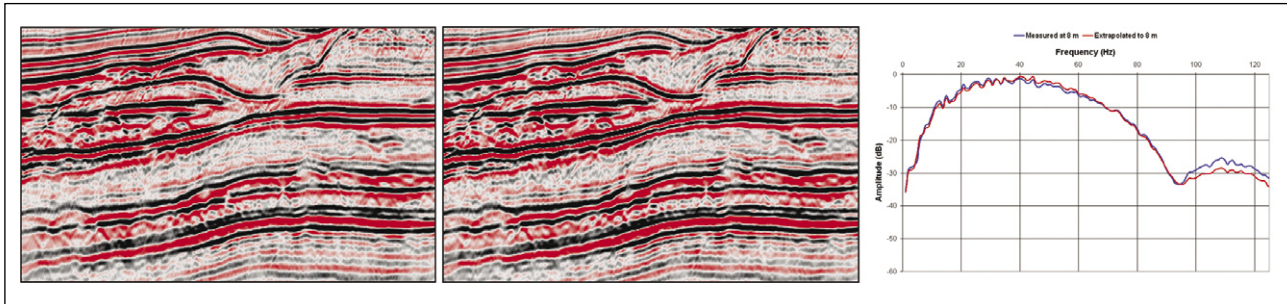


Figure 4 The images are from left to right, the hydrophone (pressure) stack acquired at 8 m depth (blue curve at right), the equivalent total pressure stack at a simulated depth of 8 m derived from the dual-sensor data acquired at 15 m depth (red curve at right), and the comparative amplitude spectra.

this depth the cable is in a quiet and stable environment.

Pre-processing of the dual-sensor data is relatively straightforward to yield the deghosted pressure and velocity wavefields. First, the impulse response of the velocity sensor (which has a non-flat spectrum) is matched to the flat zero phase hydrophone spectrum. This step takes into account the difference in the sensitivities between the two sensors.

Velocity sensor data over the range of 0 - 20 Hz are predicted from the pressure sensor data using the mathematical formulation given above. This is desirable because velocity sensors record strong low-frequency mechanical noise. The conditioning of the low-end frequency range is mathematically robust for scattered wavefields (the direct arrivals are removed); and as frequencies less than 20 Hz have wavelengths longer than 75 m, small errors in streamer depth or small departures from a flat sea surface have little effect on the conditioning process.

The dual-sensor data is then separated into up-going and down-going pressure and velocity wavefields using angle-

dependent methods similar to those for ocean bottom seismic processing (Ikelle and Amundsen, 2005).

After being separated into up-going and down-going components, both pressure data and particle velocity data can be extrapolated to any desired recording depth. Thereafter, the data are passed on to a ‘conventional’ processing flow, modified of course to exploit and preserve the improved frequency and signal-to-noise content of the signal.

Figure 4 is a processing QC/verification that compares a large data window and superimposed amplitude spectra for the following:

- Conventional pressure-only streamer towed at 8 m depth
- Dual-sensor streamer towed directly below at 15 m depth
- Low frequency velocity data conditioning over 0 - 20 Hz
- Wavefield separation into up-going and down-going pressure wavefields
- Extrapolation of both (separated) wavefields to 8 m depth
- Summation to yield the total pressure wavefield at 8 m depth

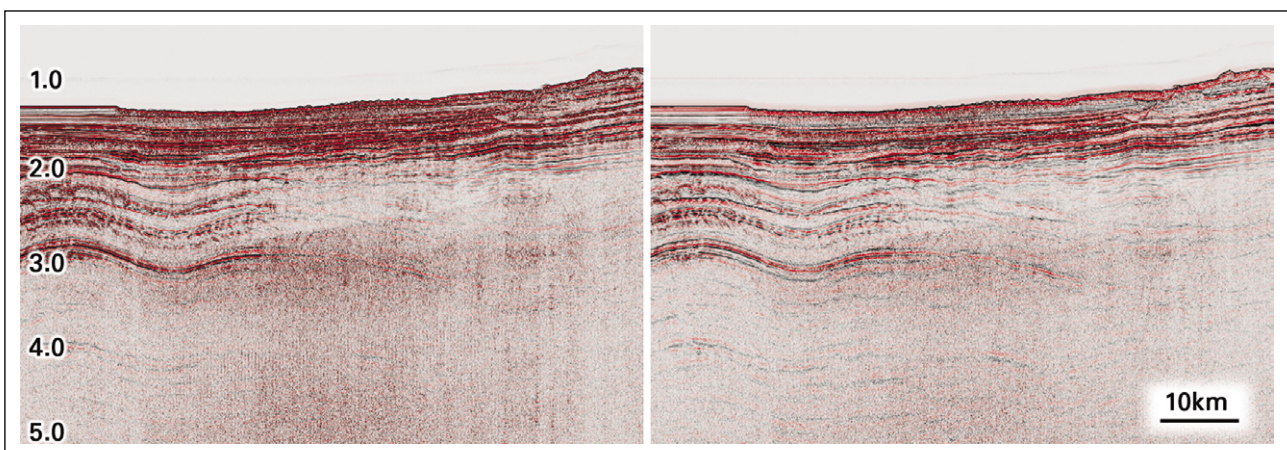


Figure 5 Unmigrated stack comparison of total pressure (ghosted) data with conventional SRME applied on the left vs. up-going (de-ghosted) pressure data from a dual-sensor streamer with an advanced dual-sensor SRME solution applied on the right. Note the improved resolution (de-ghosted), increased signal-to-noise content, and reduced noise and multiple content on the right. Weak primary events on the left are now easily and robustly interpreted in the dual-sensor result.

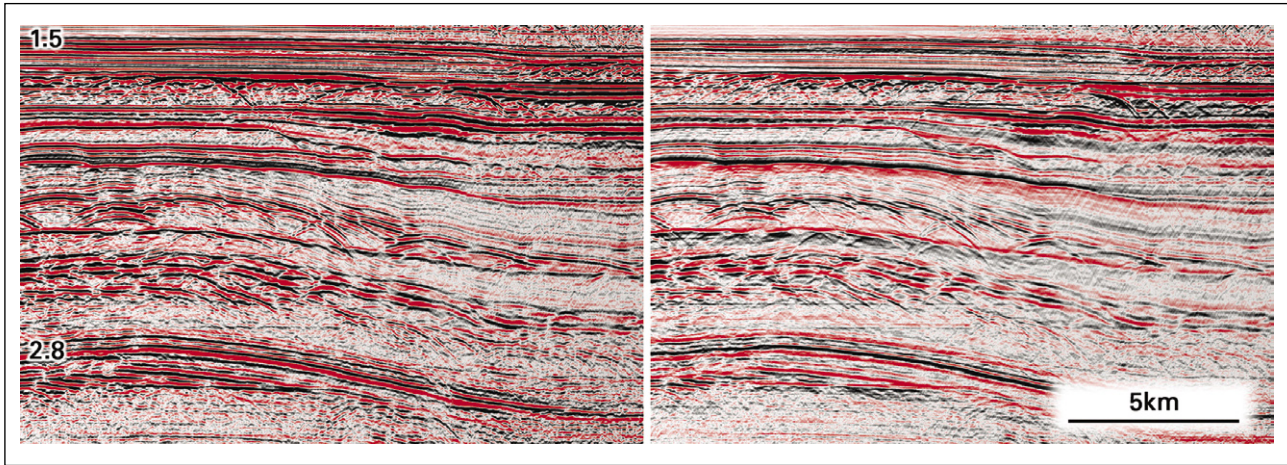


Figure 6 An unmigrated total pressure stack from a conventional streamer (receiver-side ghost included) on the left vs. the de-ghosted up-going pressure result from a dual-sensor streamer on the right. Data processing was used to yield an effective receiver depth of 8 m for both results.

The results in Figure 4 show that the reconstructed total pressure wavefield from the dual-sensor data and the recorded total pressure wavefield are essentially identical (as expected), including the frequency spectra at very low frequencies. This (consistent) observation supports the accuracy of the low frequency velocity data conditioning, and the integrity of the other pre-processing steps.

A further advantage arising from the ability to separate wavefields is that an advanced implementation of surface related multiple elimination (SRME) is possible (Söllner et al., 2007 - Fig. 5). Multiple prediction is based on the up-going pressure wavefield and the down-going velocity wavefield extrapolated to the source level so that the kinematics of surface-related multiples are accurately represented. The key advantage of using the down-going velocity wavefield is that

any variations in the sea surface level and reflection coefficient are implicitly included in the prediction. In addition, the use of a particle velocity field automatically incorporates a necessary angle-dependent scaling into the prediction process.

Increased penetration and signal-to-noise content

Figures 6 to 9 present several dual-sensor data examples from two different survey locations in the North Sea. In both cases a conventional hydrophone-only streamer was towed at a depth of 8 m, and a dual-sensor streamer was towed below the conventional streamer at a depth of 15 m. This allowed a spatial correlation and verification between the two recorded datasets. Figures 6 and 7 address data acquired with 6100 m streamers, and Figures 8 and 9 address data acquired with 8100 m streamers. Data processing followed the fundamental

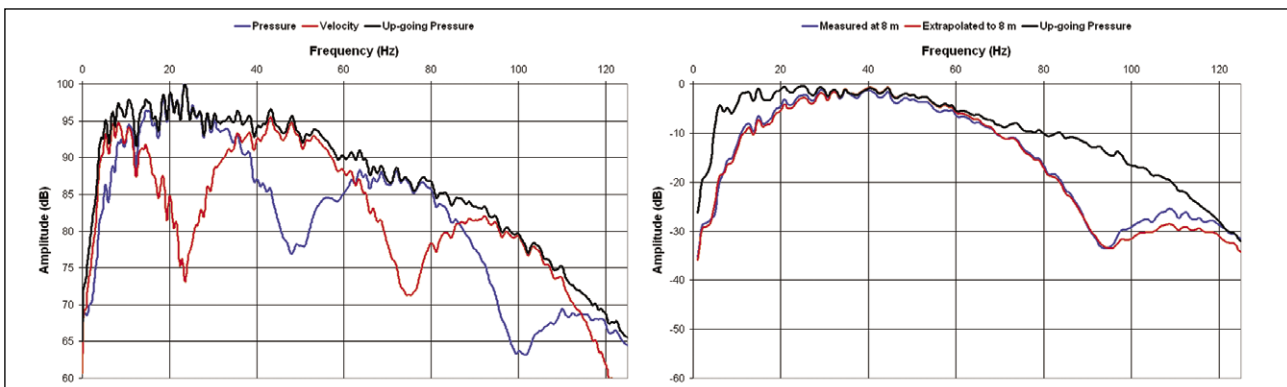


Figure 7 The figure on the left is a superposition of the amplitude spectra for the total pressure (ghosted) wavefield (blue), the velocity wavefield (red), and the de-ghosted up-going pressure wavefield (black). The dual-sensor data were acquired at a streamer depth of 15 m (refer also to Fig. 3). The figure on the right is a superposition of the amplitude spectra for the total pressure (ghosted) wavefield recorded at a depth of 8 m (blue), the processed total pressure (ghosted) wavefield at a depth of 8 m but derived from dual-sensor data recorded at a depth of 15 m (red), and the de-ghosted up-going pressure wavefield (black). Note the significant boost in low and high frequency amplitudes for the de-ghosted result (refer also to Fig. 4).

Marine Seismic

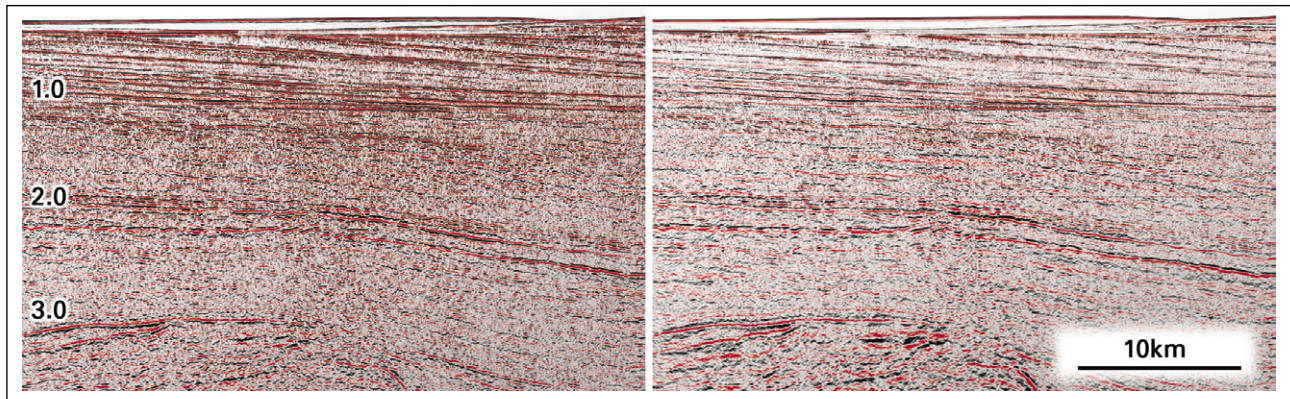


Figure 8 A migrated total pressure stack from a conventional streamer (receiver-side ghost included) on the left vs. the de-ghosted up-going pressure result from a dual-sensor streamer on the right. Data processing was used to yield an effective receiver depth of 8 m for both results. Note the significantly increased data resolution and clarity on the right. The amplitude and character of deeper events is also significantly improved on the right.

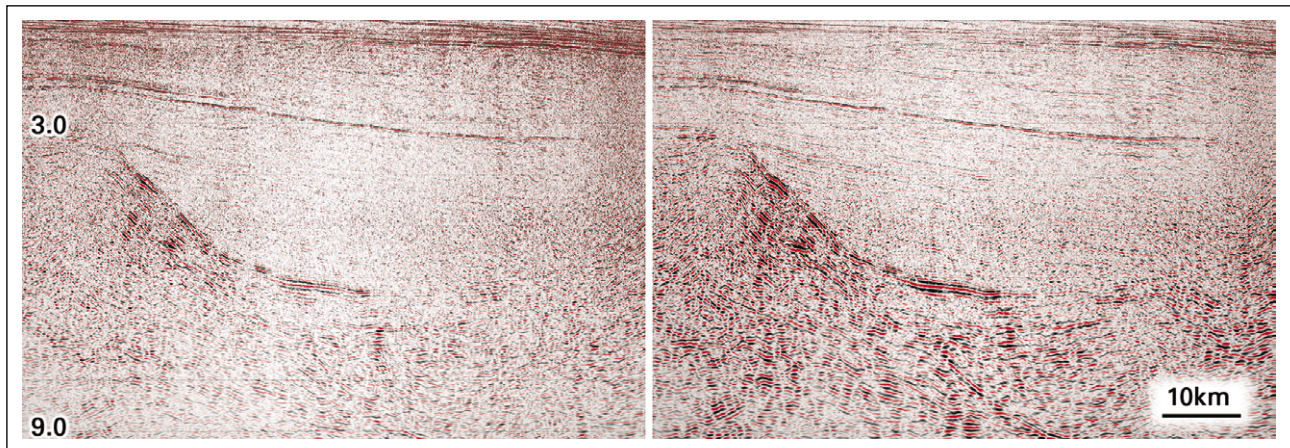


Figure 9 A deeper windowed version of Figure 8. Deep basement features and intra-sedimentary events become strikingly evident on the right.

principles discussed above, and demonstrates the significant improvements provided by the up-going pressure wavefield in terms of event resolution, frequency content, deep target penetration, and increased signal-to-noise content with a dual-sensor streamer.

Figure 6 presents a data window 1 to 2 s TWT below the water bottom. Data processing is deliberately simplistic in an effort to highlight the fundamental benefits of dual-sensor streamer acquisition and processing. Note the complete removal of the receiver-side ghost on the right side of Figure 6. The total event set is effectively halved resulting in a more interpretable, less ambiguous image. Figure 7 revisits the benefit of de-ghosting to the amplitude spectra, both in terms of boosting low and higher frequencies normally lost because of the receiver ghost, and in terms of boosting the low frequency content because of towing deep at 15 m. In a dual-sensor streamer, towing deep invokes no penalty to the higher frequencies. Furthermore, signal-to-noise content on both the pressure and velocity

wavefields is excellent, as is the de-ghosted up-going pressure wavefield derived during data processing.

Figure 8 presents a data window over the first 3 s TWT below the water bottom. In addition to better data resolution and frequency content at all depths with the dual-sensor data, deep event amplitude and character improves significantly from de-ghosting and because of towing deep at 15 m. Finally, Figure 9 presents a data window over the first 8 s TWT below the water bottom (record length was 10 s). Note the profound improvement in deeper data event amplitude and character with the dual-sensor data.

In terms of operational efficiency, towing a deep dual-sensor streamer allows operations in an extended weather window, sometimes in scenarios where conventional operations would be shut down. Efficient acquisition follows from towing all streamers with collocated pressure and velocity sensors at one depth, exploiting the full streamer width capacity of the vessel, and easily controlling all streamer behaviour.

Conclusions

A new dual-sensor streamer records both pressure and the vertical component of the particle velocity. Separation into up-going and down-going pressure and velocity wavefields is straightforward. Thus, the receiver ghost can be completely removed from the pressure wavefield, increasing data resolution. The related seismic data is more reliable to interpret, and contains greater frequency bandwidth and greater signal-to-noise content than can be obtained using conventional streamers that record only the pressure field. Furthermore, deeper target amplitudes are stronger and more continuous.

Deep streamer towing increases the operational weather window, reduces noise, and increases signal penetration. Pressure and velocity are measured at collocated locations, using all streamers towed at the same depth. Towing all streamers at one depth optimizes operational efficiency and improves data integrity. The dual-sensor streamer technology described here creates several new opportunities for advanced multiple removal, seismic inversion, and data interpretation.

References

- Amundsen, L. [1993] Wave-number-based filtering of marine point source data. *Geophysics*, 58, 1335-1348.
- Barr, F.J. and Sanders, J.I. [1989] Attenuation of water-column reverberations using pressure and velocity detectors in water-bottom cable. *Annual Meeting Expanded Abstracts*, SEG, 653-656.
- Carlson, D., Söllner, W., Tabti, H., Brox, E., and Widmaier, M. [2007] Increased resolution of seismic data from a dual-sensor streamer cable. *Annual Meeting Expanded Abstracts*, SEG, 994-998.
- Claerbout, J.F. [1976] *Fundamentals of geophysical data processing*. Blackwell Science, 274 pp.
- Fokkema, J.T. and van den Berg, P.M. [1993] *Seismic applications of acoustic reciprocity*. Elsevier, Amsterdam, 350 pp.
- Ikelle, L.T. and Amundsen, L. [2005] Introduction to petroleum seismology. *SEG Investigations in Geophysics Series No. 12*, 679 pp.
- Schneider, W.A. and Backus, M.M. [1964] Ocean-bottom seismic measurements off the California Coast. *J. Geophys. Res.*, 69, 1135-1143.
- Söllner, W., Brox, E., Widmaier, M., and Vaage, S. [2007] Surface-related multiple suppression in dual-sensor towed-streamer data. *Meeting Expanded Abstracts*, SEG, 2540-2544.
- Tenghamn, R., Vaage, S., and Borresen, C. [2007] A dual-sensor, towed marine streamer; its viable implementation and initial results. *Annual Meeting Expanded Abstracts*, SEG, 989-993.